

Electronic Supplementary Information

Unraveling The Crucial Role of Spacer Ligand in Tuning

Contact Properties in Metal–2D Perovskite Interfaces

Zhuo Xu^{a*}, Ming Chen^d and Shengzhong Frank Liu^{a,b,c*}

^aKey Laboratory of Applied Surface and Colloid Chemistry, National Ministry of Education; Shaanxi Key Laboratory for Advanced Energy Devices; Shaanxi Engineering Lab for Advanced Energy Technology; Institute for Advanced Energy Materials; School of Materials Science and Engineering, Shaanxi Normal University, Xi'an 710119, China.

^bDalian National Laboratory for Clean Energy; Dalian Institute of Chemical Physics, Chinese Academy of Sciences, Dalian 116023, China.

^cUniversity of the Chinese Academy of Sciences, Beijing 100039, China.

^dCollege of Physics and Electronics Engineering, School of Electric Power, Civil Engineering and Architecture, State Key Laboratory of Quantum Optics and Quantum Optics Devices, Shanxi University, Taiyuan, China, 030006.

*E-mail: xuzh@snnu.edu.cn (Z.X.)

*E-mail: szliu@dicp.ac.cn (S.L.)

METHODS

In this study, the DFT calculations were performed using the Vienna Ab initio Simulation Package (VASP). The projected augmented wave (PAW) pseudopotentials and the PBEsol exchange-correlation functional within the generalized gradient approximation (GGA) were employed. An energy cutoff of 500 eV was set for the plane-wave function's expansion. The van der Waals (vdW) dispersion correction was found necessary to yield more accurate lattice constants, which are described by the DFT-D3 correction. The optimization of the bulk PEA_2PbI_4 lattice structure is performed by applying Monkhorst-Pack sampling with a Γ -centered $5\times 5\times 3$ k-point grid. The lattice parameters and atomic positions of bulk PEA_2PbI_4 were relaxed until the total energy changes were less than 1.0×10^{-5} eV and the maximum force component acting on each atom was less than 0.01 eV \AA^{-1} . Then, the slab models of monolayer PEA_2PbI_4 are cleaved from the bulk structure along the stacking direction. While the initial unit structure of $\text{PEA}_2\text{MAPb}_2\text{I}_7$ and $\text{PEA}_2\text{MA}_2\text{Pb}_3\text{I}_{10}$ are constructed by appropriately placing the PEA^+ ligands at both ends of two and three layers of corner-sharing PbI_6 octahedra, respectively, which are obtained by cutting out tetragonal MAPbI_3 unit cells along the $[001]$ direction to reduce the number of PbI_6 octahedra layers. For the contact simulation, a periodic boundary condition is applied along the in-plane direction, and a vacuum spacing >20 \AA is set along the direction perpendicular to the interface to avoid the interaction between periodic cells in the stacking direction. For the construction of metal- PEA_2PbI_4 interfaces, Al, Ag, Ir, Au, Pd, and Pt substrates that cover a wide range of WFs are used, forming a suitable system for a systematic study of the band level alignment in metal- PEA_2PbI_4 interfaces. To form better interfacial lattice matching and minimize the interfacial stress, $2\times 2\times 1$ supercell of PEA_2PbI_4 is matched with a $3\sqrt{2}\times 3\sqrt{2}\times 1$ supercell of the metal $[001]$ slab. For consistence, the in-plane lattice constants of all metal- $\text{PEA}_2\text{MA}_{n-1}\text{Pb}_n\text{I}_{3n+1}$ ($n = 1, 2, \text{ and } 3$) slabs are fixed in consistence with that of

PEA₂PbI₄. Thus, maximum tensile strains of 4.7% for Ir and compressive strain of 2.7% for Au are applied among the six metals, as shown in Table 1. A Γ -centered k-point sampling of $2 \times 2 \times 1$ is used for contact calculation. All the contact structures are relaxed until the total energy and maximum force component acting on each atom are 1.0×10^{-5} eV and 0.02 eV \AA^{-1} , respectively.

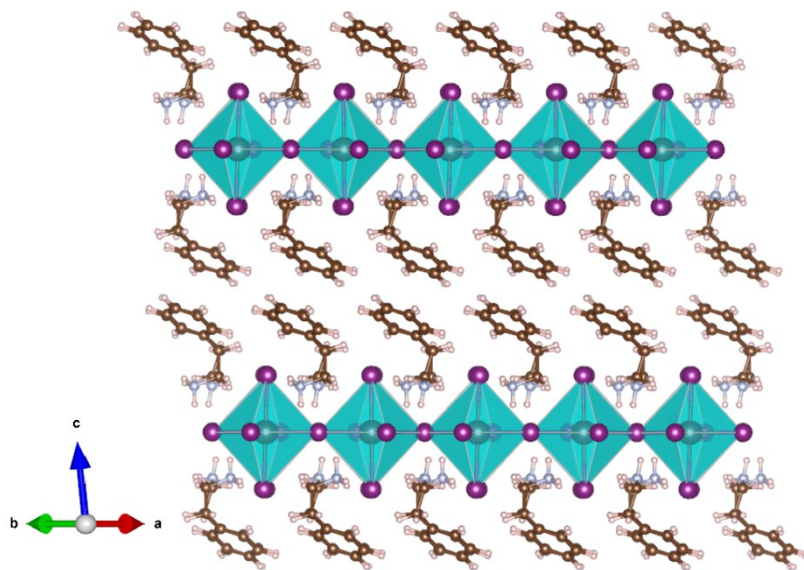


Fig. S1. Structural configurations of PEA₂PbI₄.

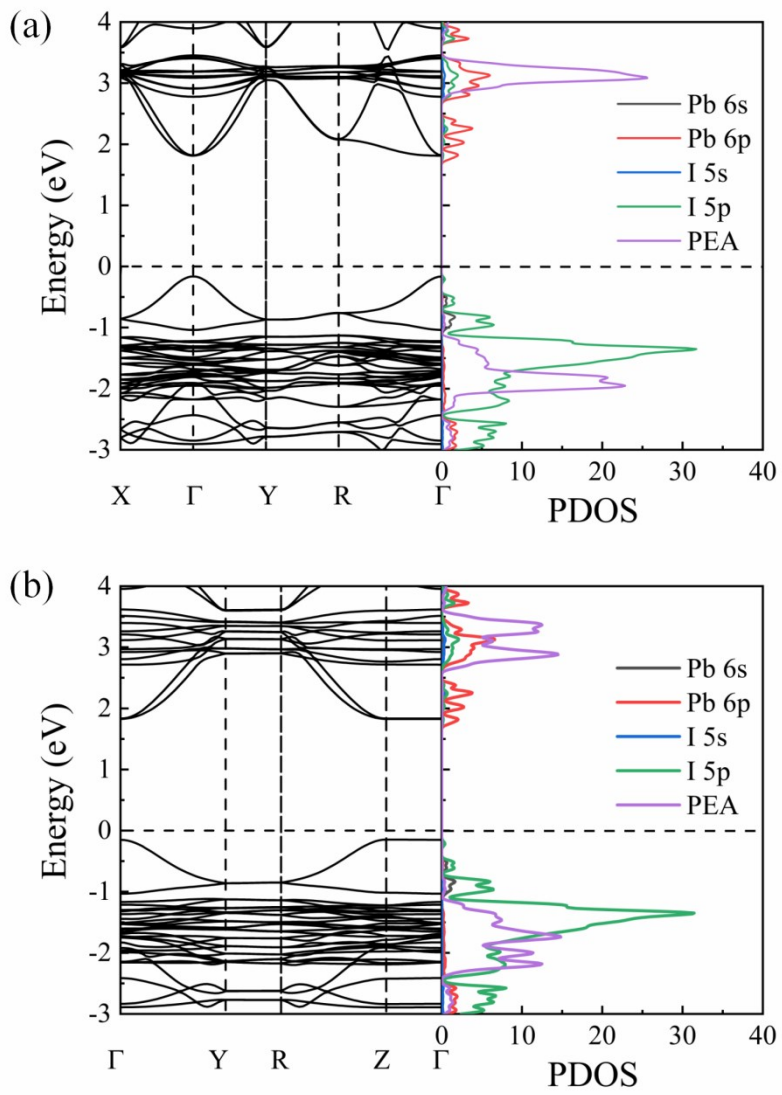


Fig. S2. Band structures and corresponding density of states for (a) bulk PEA_2PbI_4 and (b) monolayer PEA_2PbI_4 .

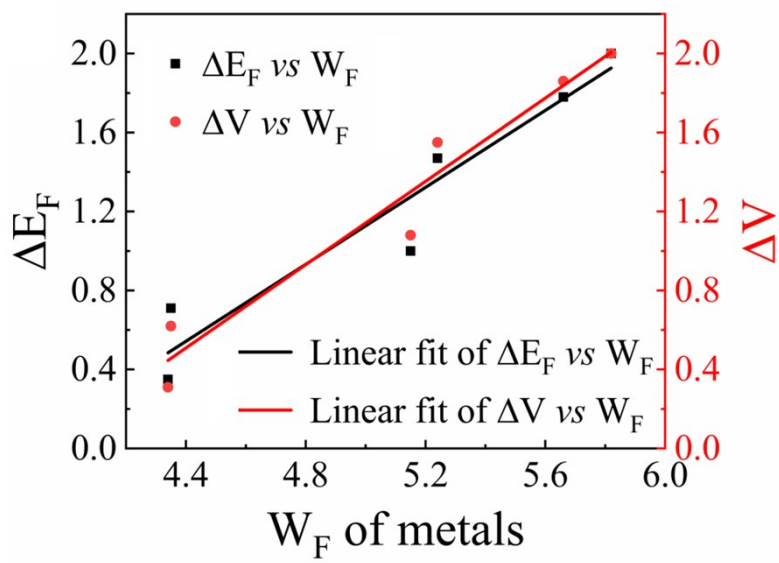


Fig. S3. Variation of potential step, ΔV , and Fermi level shift, ΔE_F , with W_F of metals.

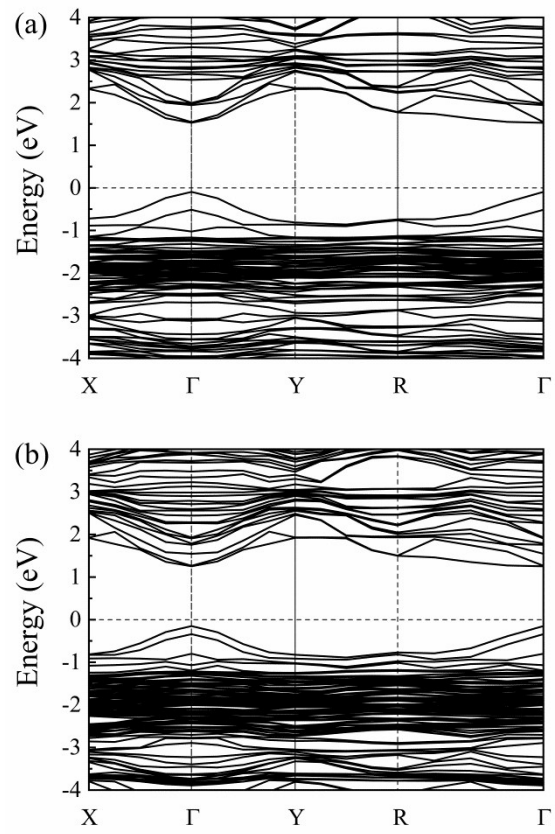


Fig. S4. Band structures of (a) $\text{PEA}_2\text{MAPb}_2\text{I}_7$ and (b) $\text{PEA}_2\text{MA}_2\text{Pb}_3\text{I}_{10}$.

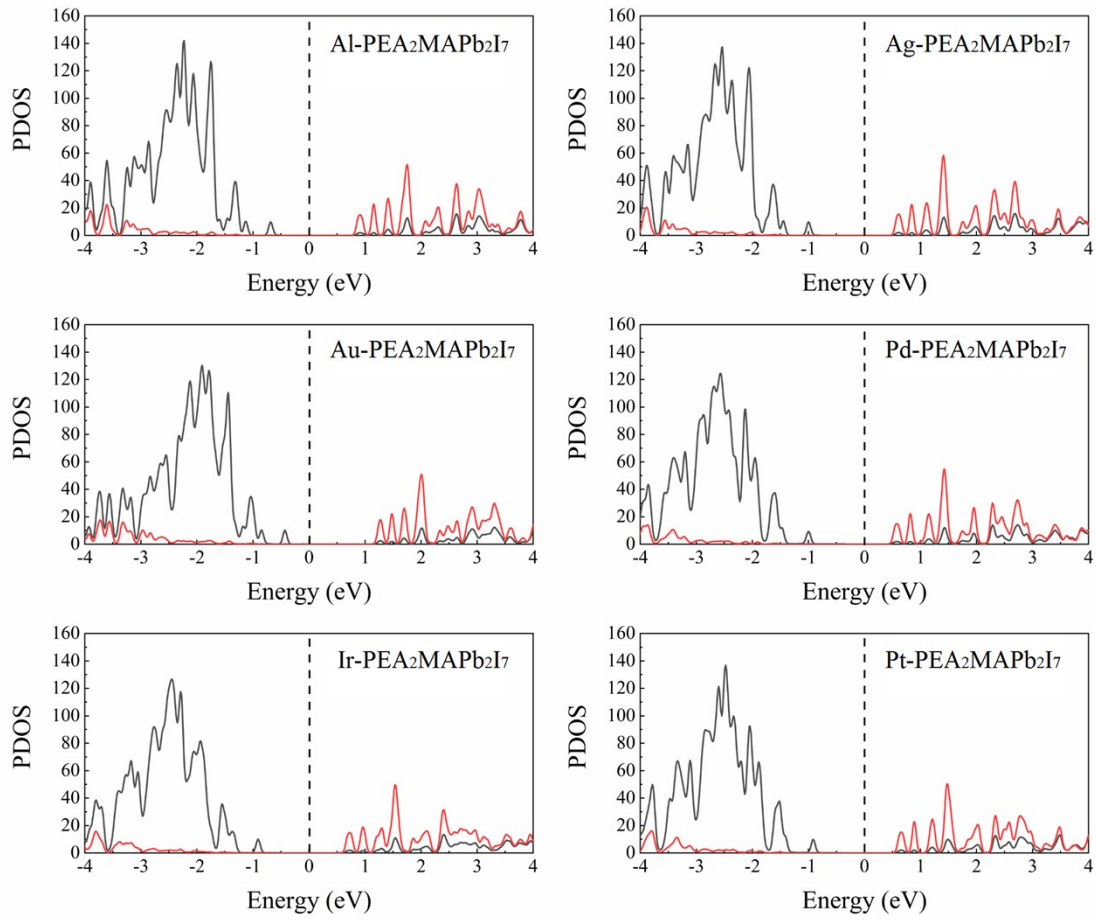


Fig. S5. Projected density of states for I 5p (dark line) and Pb 6p (red line) orbitals in all six metal- $\text{PEA}_2\text{MAPb}_2\text{I}_7$ contacts.

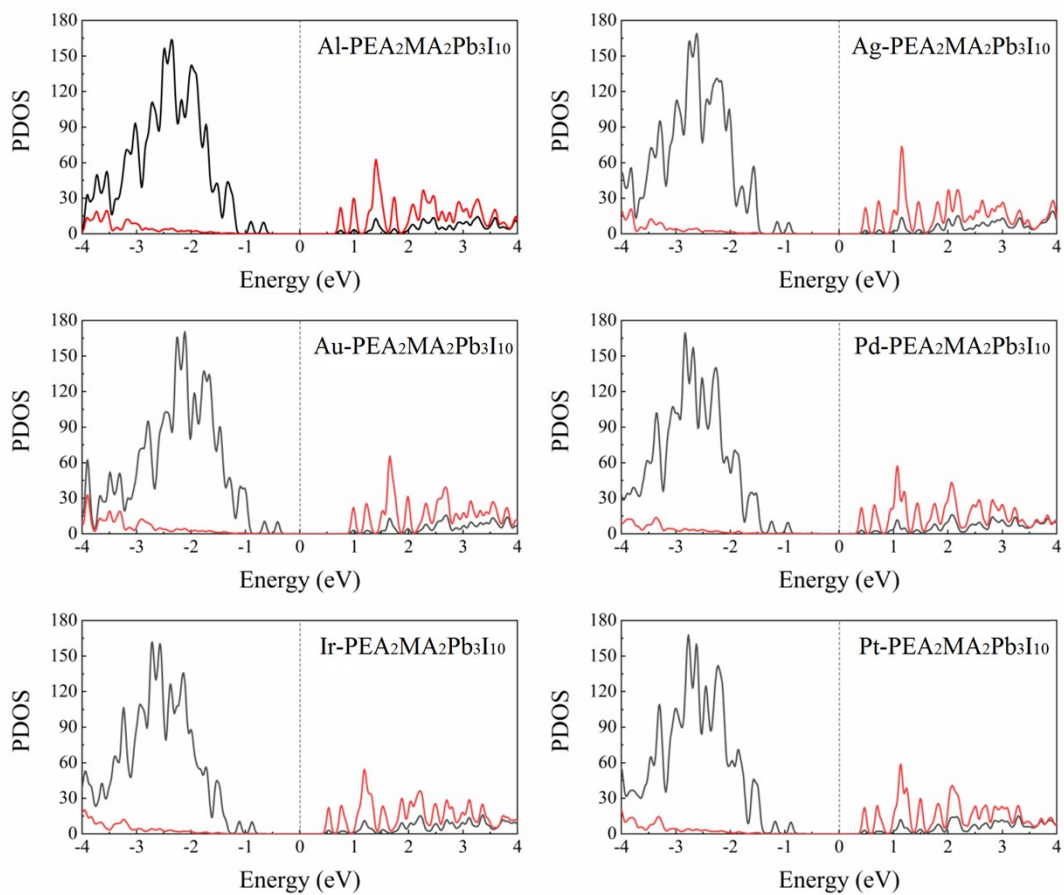


Fig. S6. Projected density of states for I 5p (dark line) and Pb 6p (red line) orbitals in all six metal- $\text{PEA}_2\text{MA}_2\text{Pb}_3\text{I}_{10}$ contacts.

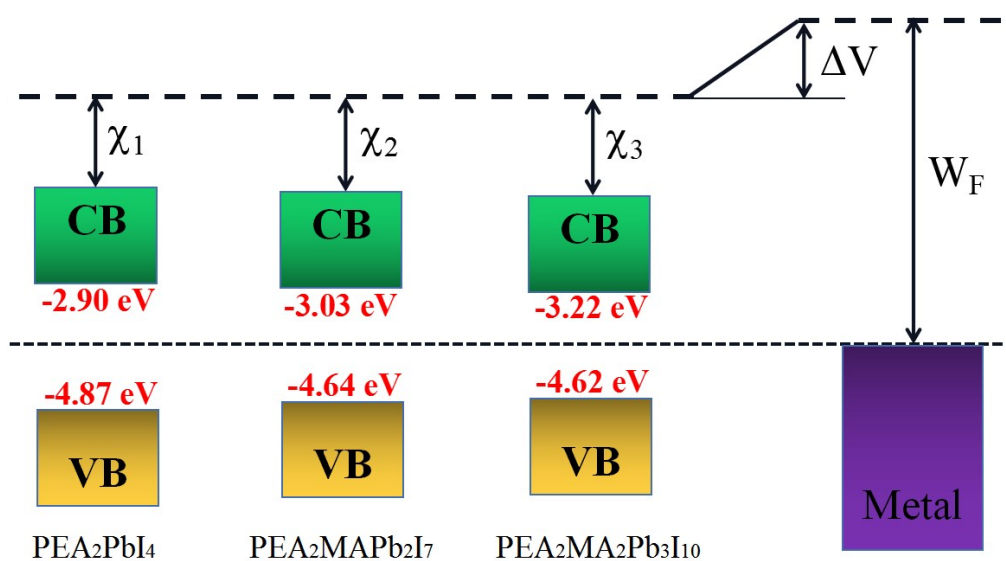


Fig. S7. Schematic illustration of the energy diagram at the interface of metal-PEA₂PbI₄, -PEA₂MAPb₂I₇, and -PEA₂MA₂Pb₃I₁₀, with χ_1 , χ_2 , and χ_3 the electron affinities of PEA₂PbI₄, PEA₂MAPb₂I₇, and PEA₂MA₂Pb₃I₁₀, respectively.